Reaction Constants for $T^3(p,n)He^3$

G. A. JARVIS, A. HEMMENDINGER, H. V. ARGO, AND R. F. TASCHEK
Los Alamos Scientific Laboratory, Los Alamos, New Mexico*
(Received March 6, 1950)

Measurements of the differential and total cross sections for $T^3(p,n)He^3$ between the reaction threshold at 1.019 Mev and 2.49 Mev are reported. At the higher energies the neutron emission in the center-of-mass system is highly asymmetric and the energy dependence of the coefficients of a cosine expansion fit to the angular distribution is determined. Evidences for resonance effects are observed at the highest proton energies used, indicating an excited state in the continuum of the intermediate He^4 nucleus. The use of the reaction as a neutron source is discussed.

I. INTRODUCTION

A PRELIMINARY investigation of the interaction of protons with tritium[1] has shown that the neutron yield of $T^3(p,n)He^3$ is large and varies rapidly with proton energy.

The results previously reported were obtained with a small scattering chamber as the target. The design of the latter was such that rather large amounts of metal were irregularly spaced about the gas volume of the target, making it unsuitable for precise neutron yield measurements. To avoid this difficulty a thin-walled gas target has been built and used in connection with the Los Alamos electrostatic accelerator to make a detailed study of the angular distributions of the neutrons from the reaction $T^3(p,n)He^3$ from the threshold[2] at 1019 kev up to 2800-kev proton energies. The McKibben nomograph[3] for this reaction may be of help in the following discussion.

II. APPARATUS

The essential features of the tritium gas target are shown in Fig. 1. Its gas volume is about 2 cm^3. The proton beam from the electrostatic accelerator, limited by the three beam-defining diaphragms *A*, *B*, and *C*, enters the thin-walled target chamber through the thin aluminum window at *C*. The target volume is electrically insulated from the beam tube by Bakelite bushings as shown in the diagram. The Kovar filling tube has a short glass section to isolate the target electrically from the gas handling system. A barrier voltage of minus 300 volts applied to the diaphragm *B* serves to prevent electrons, coming backwards from the aluminum window, from escaping the target. Protons can strike only the window and not the diaphragm on entering the gas volume. With the retarding voltage on *B* no measurable change in current occurred when a magnetic field was applied across the gas volume, indicating that an accurate measurement of charge collected was being made. The proton current integral entering the target was measured within ± 0.2 percent with a Gittings-type current integrator.[4]

The gas handling system, Fig. 2, has been considerably simplified over the earlier arrangement.[1] The volume of the filling system is kept to a minimum by using $\frac{1}{8}''$ bore quartz tubing for the UT_3 storage tube, $\frac{1}{8}''$ bore Pyrex tubing for the mercury manometer and $\frac{1}{16}''$ bore Kovar tubing for the interconnecting leads. Likewise, the stainless steel needle valves were made to have small volumes. With this arrangement, the target can be filled to any pressure up to about an atmosphere by direct evolution from the tritium storage tube. This maximum pressure is limited by the design of the manometer and the breaking strength of the target windows, rather than by the thermal decomposition properties of UT^3.

The neutron yields were measured with two flat-response long counters.[5] One of these remained at a fixed angle and distance from the target and served primarily as a monitor for determining relative yields during the measurement of a given angular distribution at a particular energy. No provision was made for closing off the target filling tube at the target, so that it was necessary to measure the change in density of tritons in the target due to heating when the protons passed through it. Since the target gas was exposed to

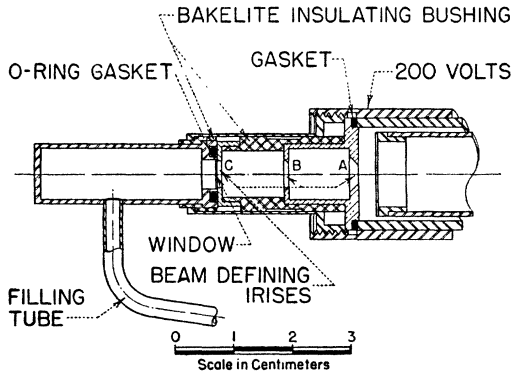

FIG. 1. Thin-walled gas target.

* This document is based on work performed at the Los Alamos Scientific Laboratory of the University of Californa.

[1] Taschek, Jarvis, Hemmendinger, Everhart, and Gittings, Phys. Rev. **75**, 1361 (1949).

[2] Taschek, Argo, Hemmendinger, and Jarvis, Phys. Rev. **76**, 325 (1949).

[3] Hanson, Taschek, and Williams, Rev. Mod. Phys. **21**, 649 (1949). For laboratory use large nomographs can be obtained from Document Sales Agency, U. S. Atomic Energy Commission, P. O. Box 62, Oak Ridge, Tennessee, as MDDC 223.

[4] H. T. Gittings, Rev. Sci. Inst. **20**, 325 (1949).

[5] A. O. Hanson and J. L. McKibben, Phys. Rev. **72**, 673 (1947).

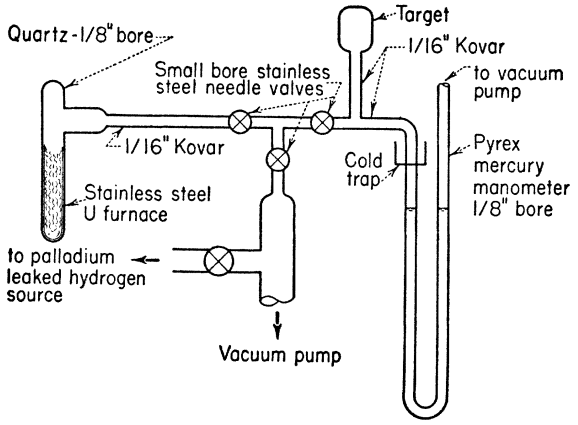

FIG. 2. Gas handling system.

the mercury manometer, heating of the target was accompanied by an actual change in the volume occupied by the tritium gas.

The second counter was mounted on a truck and pivoted to move in a circle about the center of the target. The distance from the center of the target to the counter face was 142″, corresponding to a subtended half-angle of about 4°.

Counter sensitivities were determined by placing a standard Ra—Be neutron source[6] at the target position and observing the counting rates. The calibration of the standard source is known within ±5 percent. The differential cross sections can be determined from the following considerations: $n(\theta)=\sigma(\theta).N_t l n_p$, where $n(\theta)$ = number of neutrons/steradian-microcoulomb intercepted by counter at θ; $\sigma(\theta)$ = differential cross section for reaction in cm²/steradian; N_t = number of tritons/cm³; l = length of proton path through target gas in cm; n_p = number of protons/microcoulomb passing through target. Now also $n(\theta)=QC'/4\pi C$, where Q = total number of neutrons/minute from the standard Ra—Be source; C = number of counts/minute of long counter using Ra—Be source; C' = number of counts/microcoulomb of long counter using $T^3(p,n)$ reaction. Combining these two expressions we get

$$\sigma(\theta)=QC'/4\pi CN_t l n_p.$$

No corrections are made for the small change in counter sensitivity over the total neutron energy range involved here.

The tritium content of the gas sample was determined from observations on proton-proton scattering[1] just previous to installing the thin-walled neutron target. The concentration was found to be 72±2 percent of tritium. An immediate measurement of the neutron yield was then made at a fixed proton energy. After the neutron target was in place any changes in the tritium content of the gas could be determined in terms of the neutron yield at this particular proton energy, the long counter calibration being checked with the Ra—Be source.

The threshold for the $T^3(p,n)He^3$ reaction has been measured accurately and provided a convenient means of determining the energy lost by the protons in passing through the thin aluminum window containing the tritium gas in the target. One simply observes the apparent threshold for the appearance of forward neutrons from the tritium gas target. The proton energy for which this occurs will be greater than the real threshold by an amount corresponding to the mean energy lost by the protons in passing through the foil. The foil thickness for other incident proton energies can then be calculated from the range ratios of Parkinson *et al.*[7]

Actually there are several complicating factors which result in an appreciable uncertainty in the value of foil thickness which one obtains from such a measurement as that described above.

First, energy straggling of protons passing through aluminum window causes some spread in energy of protons entering the gas volume of the target. For the nominally 0.2-mil aluminum foils[8] used, the mean spread for this type of straggling is about 10 kev, as calculated[9] and as measured by Madsen and Venkateswarlu.[10]

Second, variations in thickness of the foil material itself undoubtedly account for a large part of the energy spread which we actually observe. Figure 3 shows $T^3(p,n)He^3$ threshold curves taken using (*A*) a thick Zr+T target, and (*B*) a tritium gas target with the protons passing through an aluminum window. For this particular 0.15-mil foil it is extremely difficult to determine the average foil thickness to better than about 10 kev.

For the angular distributions taken at energies above the 90° threshold the target was filled to approximately 5.0 cm Hg tritium gas. This corresponded to a maximum proton energy loss in the gas at threshold of about 12 kev. The target pressure was measured to the nearest 0.01 cm with a traveling microscope focused on the mercury manometer.

For the data taken below the 90° threshold the target thickness was about half of the above amount.

III. PROCEDURE

Since hydrogen was introduced into the target frequently to check on the background neutrons, the following procedure for taking data was used to mini-

[6] R. L. Walker, MDDC-414 (1945).

[7] Parkinson, Herb, Bellamy, and Hudson, Phys. Rev. **52**, 75 (1937).

[8] This rather remarkably hole-free aluminum comes in about 1-inch wide continuous ribbon on a spool, the thickness varies between 0.15 mil and 0.18 mil. The foil is manufactured by Cochran Foil Company, Louisville, Kentucky.

[9] M. S. Livingston and H. A. Bethe, Rev. Mod. Phys. **9**, 282 (1937).

[10] C. B. Madsen and P. Venkateswarlu, Phys. Rev. **74**, 1782 (1948).

mize errors arising from possible further hydrogen contamination of the tritium sample.

The movable counter was placed at zero degrees and a forward yield curve taken, using very low proton currents and suitable cooling so that errors arising from gas temperature changes were negligible. The differential cross sections for the forward yield were calculated from the expression given above. All subsequent measurements were taken relative to the neutron monitor and normalized at zero degrees to the appropriate energy point on the forward yield curve.

In taking the angular distributions much larger proton currents were used (about 4 μamp.) and consequently target heating was sufficient to cause the triton density to decrease considerably during a run, but the ratio of counts for the movable counter to monitor was independent of effects due to target heating as well as hydrogen contamination.

Background runs with hydrogen in the target were made for the various proton energies used. The background neutrons were generally negligible except at the highest proton energies where they were as high as one percent of the total. The yield of the background neutrons as a function of proton energy had about the same form as those from tritium, indicating that the observed background was largely due to tritium absorbed in the target backing.

IV. RESULTS

In Fig. 4 the differential cross section for the 0° yield is plotted as a function of proton energy from the threshold up to about 2.8 Mev. The initial peak just above threshold arises primarily from geometrical effects associated with the center of mass motion, which make the neutrons come out in a cone near threshold.[11]

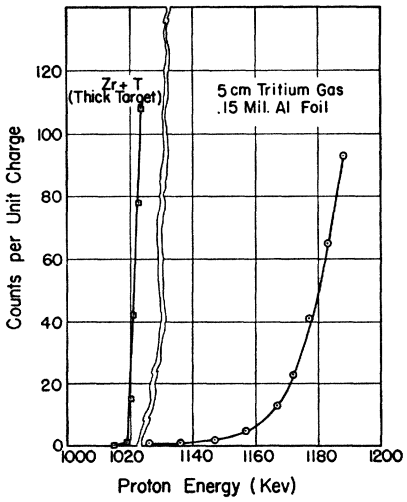

FIG. 3. Neutron yields near $T^3(p,n)He^3$ threshold taken with (a) solid target of tritium absorbed in a zirconium foil, (b) tritium gas target with beam entering target through thin aluminum window.

[11] See reference 3, p. 641.

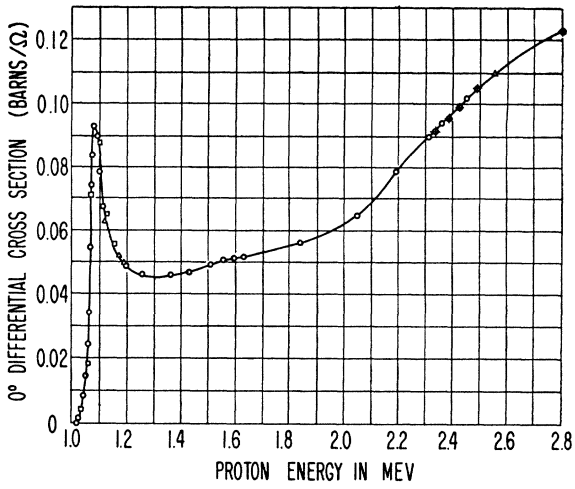

FIG. 4. Neutron yield in the forward direction plotted as a function of the incident proton energy.

It is easily shown from the relation

$$I_{\text{lab}}(\theta)d\omega_{\text{lab}}=I_{\text{c.m.}}(\phi)d\omega_{\text{c.m.}},$$

that at 0°

$$I_{\text{lab}}(0°)=2I_{\text{c.m.}}(0°)\left[1+0.1118\frac{E_p}{(E_p-E_{th})}\right],$$

where $I_{\text{lab}}(\theta)$ is the neutron intensity in the laboratory solid angle $d\omega_{\text{lab}}$ and $I_{\text{c.m.}}(\theta)$ is the intensity in the center of mass solid angle $d\omega_{\text{c.m.}}$ at angle ϕ; E_p is the proton energy and E_{th} the proton energy at the reaction theshold. Thus the solid angle transformation factor (in brackets) becomes very large as E_p approaches the threshold from above. How the laboratory yield drops to zero, rather than going to infinity, as the threshold is approached depends, of course, primarily on how $I_{\text{c.m.}}(0°)$ goes to zero, and on the secondary effects of target thickness, straggling, and counter geometry. Assuming $I_{\text{c.m.}}(0°)$ constant, the target thickness alone could account for the initial rise in the curve since the first appearance of neutrons would be from the initial negligibly thick layer of the target gas. The rise-width on this basis would be about equal to the target thickness. Actually, due to all of these effects, the observed rise-width is much greater than the target thickness.

In Fig. 5 are shown the laboratory differential cross sections for neutron production for a number of proton energies plotted as a function of the laboratory angle. For each proton energy data were recorded at 10° intervals from 0° to 120°. The number of neutron counts per datum was 5000 or more so that the statistical errors were negligible compared to the other uncertainties mentioned above.

The cross sections, measured in barns per unit solid angle, are large and make this reaction a competitor of the $Li^7(p,n)Be^7$ as a neutron source.[12] At the higher

[12] R. F. Taschek and A. Hemmendinger, Phys. Rev. 74, 373 (1948).

energies there is a larger neutron yield at back angles than for the $Li^7(p,n)Be^7$, indicating a possibly greater usefulness of $T^3(p,n)He^3$ as a neutron source for some experiments.

The angular distributions corresponding to proton energies which are less than the 90° threshold, below which all neutrons emerge in a forward cone, are shown in Fig. 6 and require some additional considerations to account for their observed shapes.

In the cone region the intensity of the slow and fast neutron groups (corresponding to neutrons ejected in the backward and the forward directions in the center of mass system) transform from the center of mass to the laboratory system according to the formula

$$I_{\text{lab}}(\theta)=I_{\text{c.m.}}{}^{f}\left(\frac{d\omega_{\text{c.m.}}}{d\omega_{\text{lab}}}\right)^{f}+I_{\text{c.m.}}{}^{s}\left(\frac{d\omega_{\text{c.m.}}}{d\omega_{\text{lab}}}\right)^{s}.$$

The superscripts s and f refer to the slow and fast neutron groups respectively, as observed at the same laboratory angle. Assuming center of mass spherical symmetry for the reaction near threshold, one finds that

$$I_{\text{lab}}(\theta)=I_{\text{c.m.}}(\phi)(d\omega_{\text{c.m.}}/d\omega_{\text{lab}})(1+E_n{}^{s}/E_n{}^{f}).$$

This function is plotted in Fig. 7 as a function of the laboratory neutron angle for two proton energies. The ratio $E_n{}^{s}/E_n{}^{f}$ always lies between unity and zero so that the factor $(1+E_n{}^{s}/E_n{}^{f})$ is not a rapidly varying function. I_{lab} is therefore dominated by the factor $d\omega_{\text{c.m.}}/d\omega_{\text{lab}}$ which has a discontinuity at the cone edge. The departures in shape of our observed angular distributions in the cone region from the type of distributions shown in Fig. 6 are believed to be due primarily to effects of the large foil straggling discussed earlier, and to a lesser extent to the target thickness and the large angle (8°) subtended by the neutron counter. Since, however, the differences between the observed and calculated angular distributions are so marked, especially at the lowest energies, it may be worth while to investigate this cone region on either this reaction, or on $Li^7(p,n)Be^7$, under more favorable conditions to assure oneself that a real effect is not being missed. If the foil difficulty can be overcome, as in solid thin Li targets, then the problem resolves itself primarily into an accurate determination of the energy dependence of the counter sensitivities. The slow group at a given angle is not too serious a problem since its intensity ratio to the fast group is the ratio of their energies.

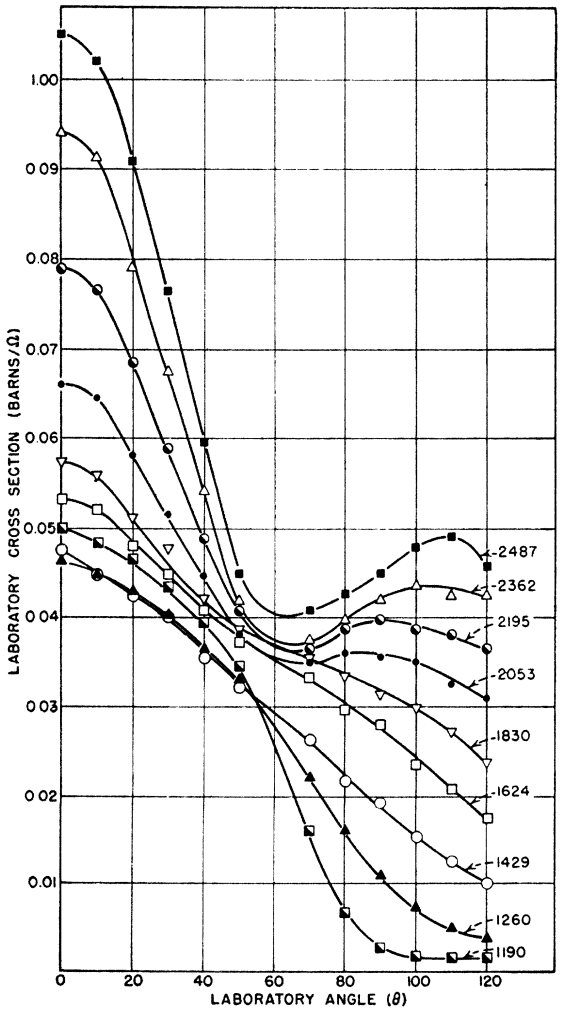

FIG. 5. $T^3(p,n)He^3$ differential cross sections in the laboratory system for proton energies above the 90° threshold. The numbers on the curves are the proton energies in kev.

The angular distributions for proton energies above the 90° threshold are not seriously affected by the foil straggling, etc., since the yields in this region have no rapid changes in intensity comparable with the cone edge discontinuities.

The maximum over-all errors in absolute differential cross sections above the threshold for neutrons at 90° laboratory angle are approximately ±10 percent and arise from the following sources:

(1) about ±5 percent in the absolute neutron yield of our Ra—Be standard source;
(2) about ±2 percent in the measurement of the concentration of the tritium in the gas sample;
(3) about ±3 percent in changes in concentration and in measuring the gas pressure in the target.

The relative errors in the angular distributions are considerably smaller than the above. For neutron energies above about 100 kev the errors are less than the 3 percent arising from uncorrected concentration changes and the measurement of target pressure. For large angles θ and low bombarding energies, i.e., below about 100-kev neutron energies, the long counter sensitivity drops in an uncertain way and here the errors in relative cross section may be as large as 10 percent.

V. CENTER OF MASS DISTRIBUTIONS

The laboratory differential cross sections for proton energies above the 90° threshold have been transformed to the center-of-mass (c.m.) system, as shown in Fig. 8, by means of the usual transformations. These curves

are calculated from *smoothed* curves through the laboratory system experimental data.

Around 1300 kev the neutron yield is seen to be approximately spherically symmetrical. However, as the proton energy is raised, an increasing fraction of the neutrons come off in the forward and backward directions, showing that higher order angular momenta strongly influence the reaction at the higher energies. The distributions are obviously not symmetrical about 90°.

VI. TOTAL CROSS SECTION

The angular distributions in the c.m. system have been fitted with a cosine series of the form

$$\sigma(\phi, E)=A(E)+B(E)\cos\phi+C(E)\cos^2\phi+D(E)\cos^3\phi.$$

Cosine cubed terms were required for a good fit of the data at the higher energies. Four fit points were used to find A, B, C, and D; the resulting expansion gave a fit that fell within the experimental errors.

The cosine series representing the c.m. angular distributions were integrated to obtain the total cross sections from

$$\sigma_{\text{tot}}(E)=2\pi\int_0^\pi \sigma(\phi)\sin\phi d\phi=4\pi[A(E)+\tfrac{1}{3}C(E)]$$

for the four terms used in the expansion. This implies an extrapolation of the c.m. yields from about 140° to 180° by means of the expansion, but the extrapolation does not produce much error in σ_{tot} since the multiplying factor $\sin\phi$ goes to zero rapidly as 180° is approached.

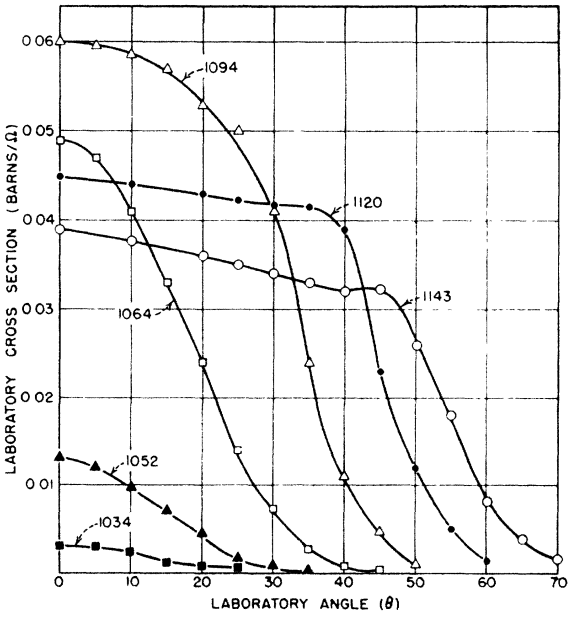

FIG. 6. $T^3(p,n)He^3$ differential cross sections in the laboratory system for proton energies below the 90° threshold. The numbers on the curves are the proton energies in kev.

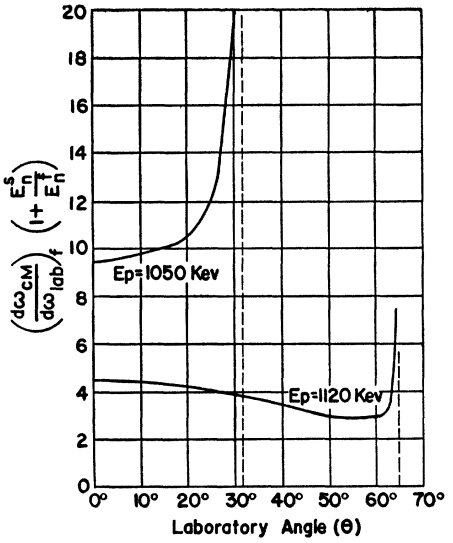

FIG. 7. Plot of the function $(d\omega_{\text{c.m.}}/d\omega_{\text{lab}})(1+E_n^s/E_n^f)$ *versus* laboratory angle for two proton energies in the cone region.

The laboratory distributions in the cone region were multiplied by $(\sin\theta)$ and integrated numerically to obtain the total cross sections. These, together with the total cross sections found above, are shown plotted in Fig. 9 as a function of proton energy. The total cross section is seen to rise rapidly from the threshold up to 2.3 Mev, the highest energy for which a complete angular distribution was taken.

Figure 10 shows the energy dependence of the coefficients in the cosine expansion used to fit the center-of-mass angular distributions. The predominant terms are clearly the angle independent S-wave term A, and C, the coefficient of $\cos^2\phi$, while B and D are considerably smaller. The C term, containing effects of P-wave protons, increases rapidly with proton energy. At the

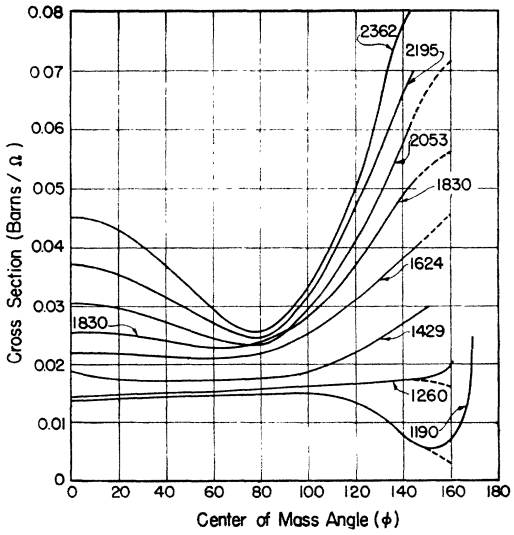

FIG. 8. $T^3(p,n)He^3$ differential cross sections in the center-of-mass system for various proton energies.

lowest energies B and D apparently change sign; this effect is probably not real, depending on the precision of the data and the functional fit. It is probable that B and D do, in fact, approach zero near the reaction threshold. No attempt has been made to fit the center-of-mass distributions with a Legendre polynomial expansion[12] since a final analysis of the data must still include spin effects.

VII. CONCLUSIONS

The data shown above on the $T^3(p,n)He^3$ reaction give some qualitative information concerning the intermediate excited nucleus He^4. The excitation energies of the He^4 lie between about 20.6 Mev and 21.6 Mev for the range of proton energies used in these experiments. This is about 1 Mev lower than the energy available to the intermediate He^4 in the $D(D,p)T^3$, but the formation of the intermediate state for $T^3(p,n)He^3$ is not hampered by the like particle selection rules of $D(D,p)T^3$.

It is immediately striking that if one considers the more reliable angular distribution data; i.e., that above the 90° threshold, only the very lowest proton energies give approximate spherical symmetry in the center-of-mass system. The asymmetry grows rapidly at 0° and 180° as the proton energy is increased, but not symmetrically around 90°. At least P-wave protons are effective in producing this asymmetry; in the $\cos\phi$ expansion fit to the center-of-mass distributions, $\cos^3\phi$ terms were found necessary, implying a finite $\cos^4\phi$ term, which, however, must have been too small to be required in the fit. In the plot of the energy dependence

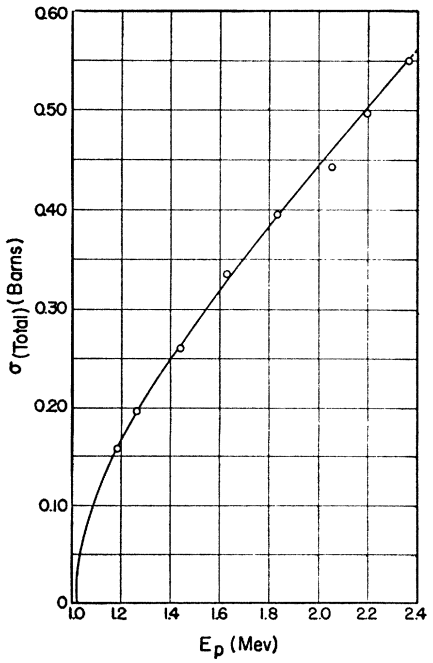

FIG. 9. Total cross sections for the reaction $T^3(p,n)He^3$ as a function of proton energy.

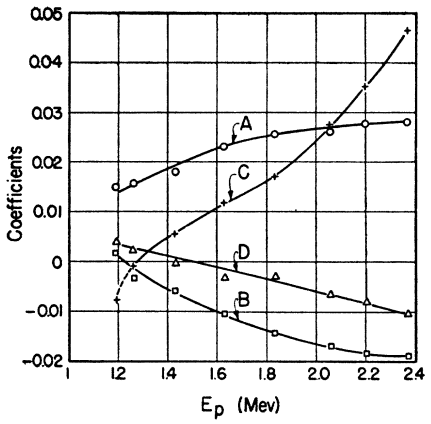

FIG. 10. Coefficients of the cosine series fits to the center-of-mass angular distributions.

of the coefficients (Fig. 10) the slope of the coefficient of $\cos^2\phi$ is increasing rapidly at the higher proton energies indicating a resonance in He^4 produced, presumably primarily by P-wave protons. Unfortunately, the maximum proton energy available was not sufficient to go over, and therefore to see such a resonance clearly. The zero degree observations show the effect rather clearly, firstly because the fraction of P wave is a maximum here, and secondly because data were obtained up to somewhat higher energies than the maximum at which a complete angular distribution was obtained. These indications of resonance effects are brought out more definitely by the observation of gamma-radiation[13] from $T^3(p,\gamma)He^4$, which places the excited state at about 2.4-Mev proton energy.

The trend of the total reaction cross section with energy (Fig. 8) does not obviously show the resonance effect discussed above because of the large admixture of S wave. If, however, one notes that even at the highest energies used here the trend of the cross section is still toward higher values, then resonance effects must be called upon to explain why leveling-off and a decrease do not appear. This argument has been made more quantitative by Dr. L. Goldstein of this laboratory who has computed the shape of the total cross section from the principle of detailed balancing using the thermal cross section[14] for $He^3(n,p)T^3$ and the assumption of its $1/v$ dependence on energy up to energies used in this experiment.

Finally, we wish to point out the usefulness of $T^3(p,n)He^3$ as a monoergic neutron source. The target techniques described above lend themselves to the use of this reaction as a rather good source down to about 150 kev, below which entrance foil straggling may become a serious limitation on energy resolution until further improvements are made in windows or in solid targets. At higher proton energies this disadvantage

[13] Argo, Gittings, Hemmendinger, Jarvis, and Taschek, Phys. Rev. 78, 691 (1950).
[14] L. D. P. King and L. Goldstein, Phys. Rev. 75, 1366 (1949). J. H. Coon and R. A. Nobles, Phys. Rev. 75, 1358 (1949).

rapidly disappears except for extremely high resolution experiments. The low threshold makes this reaction useful with accelerators for which the $Li^7(p,n)Be^7$ threshold is difficult to reach. It seems very probable that monoergic neutrons up to at least 6 Mev can be obtained with higher energy machines, since the $D(D,n)He^3$ reaction has shown no excited states in the residual He^3 nucleus to neutron energies this high; the decided advantage of $T^3(p,n)He^3$ would be, however, the low background because of proton acceleration and the large yield.

We wish to thank Messrs. H. T. Gittings and G. G. Everhart for valuable assistance in carrying out the experimental work described.

PHYSICAL REVIEW VOLUME 79, NUMBER 6 SEPTEMBER 15, 1950

Nuclear Energy Levels in Lead Isotopes*

R. E. PETERSON,† R. K. ADAIR,** AND H. H. BARSCHALL
University of Wisconsin, Madison, Wisconsin

(Received June 1, 1950)

The total neutron cross section of radiogenic lead was studied as a function of neutron energy in the range from 15 to 750 kev, using energy resolutions of 3 to 10 kev. Several resonances were observed; these were interpreted as caused by energy levels in the compound nucleus Pb^{207}. The level spacing found in Pb^{207} was of the order of 50 kev. Maxima previously found in the cross section of ordinary lead and attributed to resonance interactions of neutrons with Pb^{208} were re-investigated with better energy resolution. No resonances were observed when earlier measurements of the cross section of Bi were extended to higher energies.

I. INTRODUCTION

IN a previous measurement of the total neutron cross section of ordinary lead,[1] three distinct maxima were observed. These were attributed to the resonance interaction of neutrons with Pb^{208} to form excited states of the compound nucleus Pb^{209}. A study of these levels is of especial interest because Pb^{208} is a double closed shell nucleus consisting of 82 protons and 126 neutrons.[2] Characteristics of the compound nucleus Pb^{209} might, therefore, be compared with predictions of nuclear shell theories.

As ordinary lead consists of the isotopes Pb^{208}, Pb^{207}, Pb^{206}, and Pb^{204} in relative abundances of 52, 23, 24, and one percent, respectively, the interpretation of the resonances was complicated by the lack of knowledge of the cross sections of Pb^{206} and Pb^{207}. In the present experiment, therefore, one of the lighter lead isotopes was studied. The cross section of radiogenic lead, consisting of 88 percent Pb^{206}, nine percent Pb^{207}, and three percent Pb^{208}, was measured as a function of neutron energy from 20 to 750 kev. The experimental procedure was the same as that described earlier.[3]

II. MEASUREMENTS ON RADIO-LEAD

The variation of the cross section of radio-lead with neutron energy is shown in the upper part of Fig. 1. The different symbols represent the different energy resolutions used in the experiment, and the heights of the vertical lines through the symbols give the standard statistical errors.

Since Pb^{206} is the main constituent of the radio-lead used, the observed resonances should be due to energy levels in the compound nucleus Pb^{207}. The spacing of the levels found is of the order of 50 kev; in contrast with this, levels in Pb^{209} were previously observed to be approximately 200 kev apart.[1] Since the excitation energy in Pb^{207} in the present experiment is approximately[4,5] seven Mev and in Pb^{209}, 4.5 Mev, the variation in level density for the two lead isotopes may be explained by this difference in excitation energy.

It may be noted that several of the resonances in radio-lead appear to produce minima in the cross section. This behavior may be understood in terms of the discussion of the shape of resonances given by MacPhail.[6] His calculations show that a resonance for elastic scattering produces a minimum in the cross section when the phase shift for potential scattering approaches $-\pi/2$. On the basis of the rigid sphere model of the nucleus, the phase shift for potential scattering of s-neutrons is given by the product of the neutron wave number and the nuclear radius. Taking the nuclear radius of lead as 9×10^{-13} cm, the s-wave phase shift for 400-kev neutrons is about -1.2 radians. Since the phase shift for potential scattering of p-neutrons is small at this energy, the minima observed at 340, 380, 395, 420, and 490 kev are believed to be produced by

* This work was supported in part by the AEC and in part by the Wisconsin Alumni Research Foundation.
† Now at Los Alamos Scientific Laboratory.
** AEC Predoctoral Fellow.
[1] Barschall, Bockelman, Peterson, and Adair, Phys. Rev. **76**, 1146 (1949).
[2] M. G. Mayer, Phys. Rev. **74**, 235 (1948).
[3] Peterson, Barschall, and Bockelman, Phys. Rev. **79**, 593 (1950).
[4] Kinsey, Bartholomew, and Walker, Phys. Rev. **78**, 77 (1950).
[5] J. A. Harvey, Phys. Rev. **78**, 345 (1950).
[6] M. R. MacPhail, Phys. Rev. **57**, 669 (1940).